MODELLING OF CUTTING FORCES AND VIBRATIONS IN MACHINING PROCESSES: A REVIEW AND PROPOSAL OF THE RESEARCH DIRECTIONS

MÔ HÌNH HOÁ LỰC VÀ RUNG ĐỘNG TRONG QUÁ TRÌNH GIA CÔNG: NGHIÊN CỨU TỔNG QUAN VÀ ĐỀ XUẤT CÁC HƯỚNG NGHIÊN CỨU

Nguyen Nhu Tung[*], Hoang Tien Dung, Pham Van Dong, Do Duc Trung, Bui Van Bao

ABSTRACT

In industry, one of the most important manufacturing processes that is machining. In machining processes, two machining processes that are often used to remove the material out of workpiece are turning and milling processes. This study mainly reviews the most important issue in turning and milling process including the cutting force modelling, vibration modelling. Modeling of the cutting forces and vibrations that can be used to predict the cutting forces and vibrations in different machining processes with different cutter geometries, different workpiece materials, different cutting conditions, and different machining-tool systems. The results from prediction processes that can be applied to improve the machining quality by reducing the cutting forces, vibration, and chatter. This paper concluded with some proposed research directions for future research in machining field.

Keywords: *Modeling, Cutting Force, Vibration, Measurement System, Machining*

TÓM TẮT

Một trong những quá trình quan trọng ứng dụng trong sản xuất công nghiệp là quá trình gia công. Trong các quá trình gia công, hai phương pháp thường được ứng dụng để bóc tách vật liệu phôi để tạo thành chi tiết gia công là phương pháp tiện và phương pháp phay. Nghiên cứu này tập trung vào một số vấn đề đặc trưng chính trong quá trình tiện và quá trình phay đó là mô hình hoá lực cắt và mô hình hoá rung động. Các mô hình về lực cắt và rung động là những mô hình chung để có thể sử dụng để dự đoán lực cắt và rung động trong các quá trình gia công khác nhau với các loại dụng cụ cắt có thông số hình học khác nhau, với các loại vật liệu phôi khác nhau, với các thông số chế độ cắt khác nhau và với các hệ thống máy - công cụ khác nhau. Các kết quả dự đoán về lực cắt, rung động có thể được ứng dụng để cải tiến chất lượng của quá trình gia công bằng việc giảm lực cắt, rung động cũng như va đập trong quá trình gia công. Nghiên cứu này cũng đã để xuất một số hướng nghiên cứu quan trọng trong lĩnh vực gia công cơ khí.

Từ khóa: *Mô hình hoá, Lực cắt, Rung động, Hệ thống đo, Quá trình gia công*

1. INTRODUCTION

1.1. Cutting Force Modelling in Turning Processes

1.1.1. Cutting Force Modelling in Orthogonal Cutting Processes

The cutting operation, especially the metal cutting operation is one of the most important processes in industrial manufacturing. These operations are used to remove material from the blank. Turning, milling, and drilling are the most common metal cutting operations. The mechanical principles of all metal cutting operations are same, but maybe, their geometry and kinematics are different to each other.

Actually, in metal cutting, the most common operations are three-dimensional and complex geometry, but in order to explain the general mechanics of metal removal, the simple case of two-dimensional orthogonal cutting is often used. In orthogonal cutting, the material is removed by a cutting edge that is perpendicular to the direction of relative tool-workpiece motion as shown in Fig. 1 [1, 2].
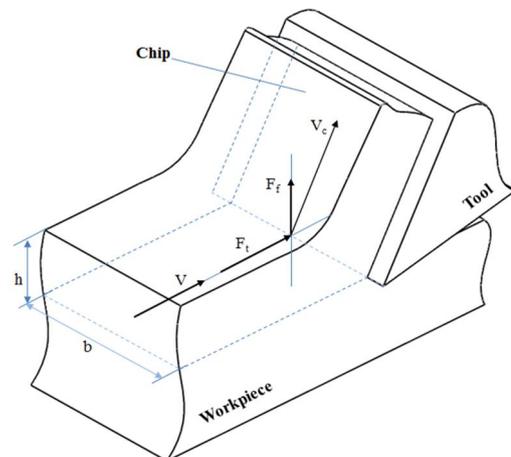
Fig. 1. Orthogonal cutting geometry [2]

The orthogonal cutting resembles a shaping process with a straight tool whose cutting edge is perpendicular to

the cutting velocity (V). A metal chip with a width of cut (b) and depth of cut (h) is sheared away from the workpiece. Assume that in orthogonal cutting, the cutting is uniform along the cutting edge; so, this is a two-dimensional plane strain deformation process without side spreading of the material. Hence, the cutting forces are exerted only in the directions of velocity and uncut chip thickness that are called tangential force (F_t) and feed force (F_f).
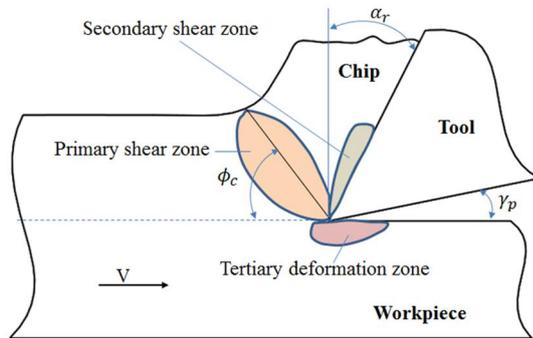
Fig. 2. Three zones in orthogonal cutting [2]

In the cross-sectional view of orthogonal cutting, there are three zones in the cutting processes as shown in Fig. 2 [2-4]. First, it is the primary shear zone. The material ahead of the tool is sheared over the primary zone to form a chip. The sheared material, the chip, partially deforms and moves along the rake face of the tool that is called the secondary deformation zone. The tertiary zone is a zone with the friction area, where the flank of the tool rubes the newly machined surface.

In orthogonal cutting process as shown in Fig. 2, the chip leaves the tool, losing contact with the rake face of the tool. The contact zone length depends on the tool geometry, tool and workpiece material, and cutting conditions such as cutting speed. Assume the cutting edge is sharp without a chamfer or radius and the deformation takes place at infinitely thin shear plane [2]. The shear angle ϕ_C that is defined as the angle between the cutting speed direction and the shear plane. It is assumed that the shear stress (τ_S) and normal stress (σ_S) are constant on the shear plane; applied at the shear plane, the resultant force (F_c) on the chip that is in equilibrium to the force (F_C) applied to the tool over the chip-tool contact zone on the rake face; assume the average friction over the chip-rake face contact zone is constant. It is assumed that the contact forces originating from the tertiary zone are equal to zero, and all cutting forces are caused by shearing process. From the force equilibrium, the resultant force (F_C) is formed from the feed cutting force (F_{fc}) and the tangential cutting force (F_{tc}), and can be calculated by Eq. (1).

$$F_c = \sqrt{F_{tc}^2 + F_{fc}^2} \qquad (1)$$

The feed force (thrust force) is in the uncut chip thickness direction and the tangential force (power force) is in the cutting velocity direction.

According to the above explanation, in orthogonal cutting process, there are three deformation zones, including primary shear zone, secondary shear zone, and tertiary deformation zone, as shown in Fig. 2. The cutting forces are explained in all cutting zones as follows:

In the Primary Shear Zone

In this zone, the shear force (F_s) acting on the shear plane that is derived from the tool and chip geometry, and it can be calculated by Eq. (2) as shown in Fig. 3.

$$F_s = F_c \cos(\phi_c + \beta_a - \alpha_r) \qquad (2)$$

where

β_a: The average friction angle between the tool's rake face and the moving chip [deg]

α_r: The rake angle of the tool [deg]

F_s: The shear force on the shear plane [N]

F_n: The normal force on the shear plane [N]
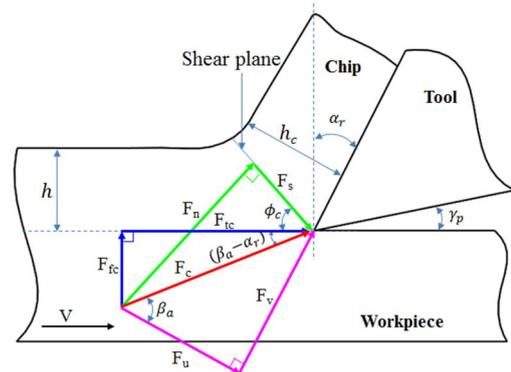
Fig. 3. Cutting forces in orthogonal cutting [2]

Besides, from cutting force diagram as shown in Fig. 3, the shear force can be expressed as a function of feed cutting force and normal cutting force as in Eq. (3).

$$F_s = F_{tc} \cos \phi_c + F_{fc} \sin \phi_c \qquad (3)$$

And the normal force acting on the shear plane can be calculated by Eq. (4).

$$F_n = F_c \sin(\phi_c + \beta_a - \alpha_r) \qquad (4)$$

or

$$F_n = F_{tc} \sin \phi_c + F_{fc} \cos \phi_c \qquad (5)$$

In the Secondary Shear Zone

In the secondary shear zone, as shown in Fig. 3, the cutting process is analyzed in the rake plane of the tool. On this plane, two components of cutting force are active: normal force (F_v) and the friction force (F_u). The normal force is calculated by Eq. (6) and the friction force is calculated by Eq. (7).

$$F_v = F_{tc} \cos \alpha_r + F_{fc} \sin \alpha_r \qquad (6)$$

and,

$$F_u = F_{tc} \sin \alpha_r + F_{fc} \cos \alpha_r \qquad (7)$$

It is assumed that in orthogonal cutting process, the chip is sliding on the tool with an average and constant friction coefficient (μ_a). In fact, the chip sticks to the rake face for a

short period and then it slides over the rake face with a constant friction coefficient [2, 5]. So, the average friction coefficient on the rake face was determined by Eq. (8).

$$\mu_a = \tan \beta_a = \frac{F_u}{F_v} \tag{8}$$

where the friction angle can be calculated from the tangential force and the feed force as by Eq. (9) and Eq. (10).

$$\tan(\beta_a + \alpha_r) = \frac{F_{fc}}{F_{tc}} \tag{9}$$

so,

$$\beta_a = \alpha_r + \tan^{-1}\frac{F_{fc}}{F_{tc}} \tag{10}$$

In the Tertiary Deformation Zone

The tertiary deformation zone is the zone where the flank of tool rubs the finished surface of workpiece. In this zone, the mechanics of cutting operation depends on the tool wear, the properties of cutting edge, and the friction characteristics of the tool and workpiece material. It is assumed that the total friction force on the flank face is F_{ff}, the force normal the flank face is F_{fn}, and the pressure (σ_f) on the flank face is uniform, the normal force on the flank face was described as in Fig. 4, and can be expressed by Eq. (11), [2, 3].

$$F_{fn} = \sigma_f.l_{fc}.b \tag{11}$$

where l_{fc} is the flank contact length, and b is the width of cut.

Assume the average friction coefficient between the flank face of tool and the finished surface is μ_f; so, μ_f can be calculated by Eq. (12).

$$\mu_f = \frac{F_{ff}}{F_{fn}} \tag{12}$$
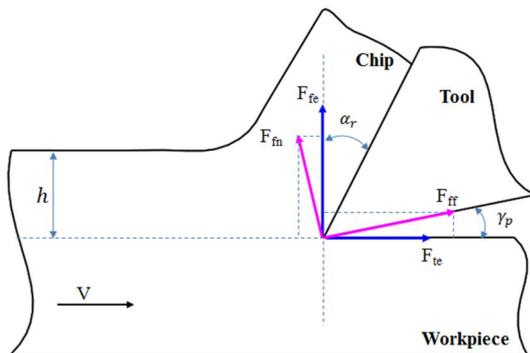
Fig. 4. The edge force in the tertiary deformation zone [2]

The angle between the flank face and the finished surface is γ_p (Clearance or relief angle). The total cutting forces can be expressed by cutting forces in tangential and feed direction as by Eq. (2.13).

$$\begin{cases} F_{te} = F_{fn} \sin \gamma_p - F_{ff} \cos \gamma_p \\ F_{fe} = F_{fn} \cos \gamma_p + F_{ff} \sin \gamma_p \end{cases} \tag{13}$$

In reality, the cutting forces are often measured in the feed and normal directions; so, the measured forces may include both shear forces (F_{tc}, F_{fc}) in the primary shear zone and secondary shear zone, and the edge forces (F_{te}, F_{fe}) in the tertiary deformation zone (ploughing or

rubbing zone). Thus, the measured cutting force components can be expressed as a superposition of shear forces and edge forces as in Eq. (2.14).

$$\begin{cases} F_t = F_{tc} + F_{te} \\ F_f = F_{fc} + F_{fe} \end{cases} \tag{14}$$

1.1.2. Cutting Force Modelling in Oblique Cutting Processes

In the oblique cutting operation, the cutting velocity is inclined at an acute angle (i) to the plane normal to the cutting edge as shown in Fig. 5. The shear deformation is plane strain without side spreading and the shearing and the chip motion are identical on all the normal planes parallel to the cutting velocity and perpendicular to the cutting edge. The resultant cutting force (F_c), along with the other forces acting on the shear and chip-rake face contact zone. The cutting force does not exist in the direction that is perpendicular to the normal plane. It is assumed that the edge force at the tertiary zone is equal to zero.
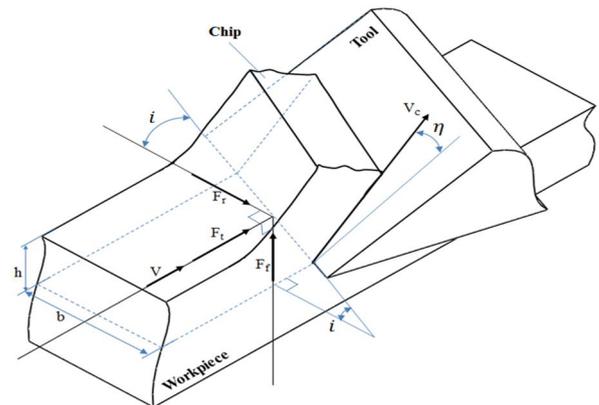
Fig. 5. The geometry of oblique cutting [2]

The cutting velocity has an oblique (inclination) angle i in oblique cutting operations. So, the directions of shear, friction, chip flow, and resultant cutting force vectors can be expressed in three Cartesian coordinate (x, y, z) as shown in Fig. 6.
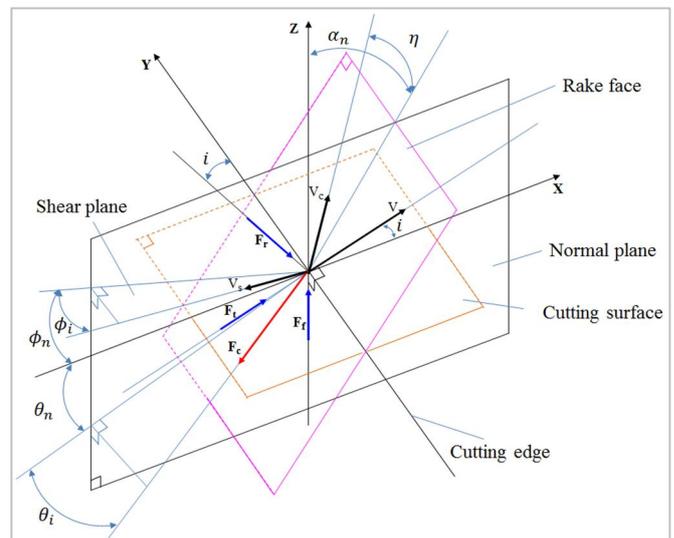
Fig. 6. Planes and angles in the oblique cutting process [2]

In oblique cutting processes, the cutting forces exist in all three directions. Assume the mechanics of oblique cutting in the normal plane are equivalent to that of orthogonal cutting; so, the normal shear angle (ϕ_n) is the angle between the shear plane and the xy plane. The oblique shear angle (ϕ_i) is the angle between the velocity vector on the shear plane and the vector normal to the cutting edge on the normal plane. The chip flow angle (η) is measured from a vector on the rake face, but normal to the cutting edge. The normal rake angle (α_n) is the angle between the z axis and normal vector on the rake face. The resultant cutting force (F_c) is formed from the friction force on the rake face (F_u) and the normal force to the rake face (F_v) with a friction angle (β_a) [2]. In the oblique cutting operation, the shear force (F_s) can be expressed as a projection of cutting force (F_c) in the shear direction by Eq. (15).

$$F_s = F_c[\cos(\theta_n + \phi_n)\cos\theta_i \text{ co } \varnothing_i + \sin\theta_i \sin\varnothing_i] \quad (15)$$

Besides, the shear foces also can be expressed as a product of shear stress and shear plane area as in Eq. (16).

$$F_s = \tau_s A_s = \tau_s\left(\frac{b}{\cos i}\right)\left(\frac{h}{\sin\varnothing_n}\right) \quad (16)$$

where A_s, b, and h are the shear area, the width of cut, and the uncut chip thickness, respectively. From Eq. (15) and Eq. (16), the cutting force can be calculated by Eq. (17).

$$F_c = bh\frac{\tau_s}{[\cos(\theta_n+\phi_n)\cos\theta_i \text{ co }\phi_i+\sin\theta_i\sin\phi_i]\cos i \sin\phi_n} \quad (17)$$

In oblique cutting processes, the measured resultant force consists of shear force (cutting force F_c) and edge force (F_e). So, the edge force components can be determined from the measured resultant force. Besides, the cutting force components can be expressed as a function of shear yield stress (τ_s), the resultant force direction (θ_n, θ_i), the oblique angle (i), and the oblique shear angle (ϕ_n, ϕ_i) as presented by Eq. (18).

$$\begin{cases} F_{tc} = F_c[\cos\theta_i \cos\theta_n \cos i + \sin\theta_i \sin i] \\ F_{fc} = F_c[\cos\theta_i \sin\theta_n] \\ F_{rc} = F_c[\sin\theta_i \sin i - \cos\theta_i \cos\theta_n \sin i] \end{cases} \quad (18)$$

So,

$$\begin{cases} F_{tc} = bh\frac{\tau_s(\cos\theta_n+\tan\theta_i\tan i)}{[\cos(\theta_n+\phi_n)\cos\phi_i+\tan\theta_i\sin\phi_i]\sin\phi_n} \\ F_{fc} = bh\frac{\tau_s\sin\theta_n}{[\cos(\theta_n+\phi_n)\cos\phi_i+\tan\theta_i\sin\phi_i]\cos i\sin\phi_n} \\ F_{rc} = bh\frac{\tau_s(\tan\theta_i-\cos\theta_n\tan i)}{[\cos(\theta_n+\phi_n)\cos\phi_i+\tan\theta_i\sin\phi_i]\sin\phi_n} \end{cases} \quad (19)$$

The measured resultant cutting forces can be written as a convenient form by Eq. (20).

$$\begin{cases} F_t = F_{tc} + F_{te} \\ F_f = F_{fc} + F_{fe} \\ F_r = F_{rc} + F_{re} \end{cases} \quad (20)$$

or

$$\begin{cases} F_{tc} = K_{tc}bh + K_{te}b \\ F_{fc} = K_{fc}bh + K_{fe}b \\ F_{rc} = K_{rc}bh + K_{re}b \end{cases} \quad (21)$$

1.2. Cutting Force Modelling in Milling Processes

1.2.1. Cutting Force Modelling with Zero Cutter Helix Angle

Milling is not only the most common processes in cutting operations, but also is very popularly employed in computer numerical control (CNC) machines for metal material removal operations. This operation is an intermittent cutting process. It is used extensively in the industrial manufacturing where both precision and efficiency are critical. In vertical three-axis milling processes, the tool (cutter) is held in a rotating spindle, while the workpiece is clamped on the table, and this table is linearly moved toward the tool. So, in milling processes, each milling tooth (flute) often traces a trochoidal path producing varying but periodic chip thickness at each tooth passing interval. However, it can be approximated by a circular path if the radius of the cutter is much larger than the feed per flute [6].

There are many milling operations such as face milling, slot milling, shoulder milling, plunge milling, ramp milling, and so on. The classification of milling operations depends on the tool geometry, workpiece geometry, cutting processes, and the machines.
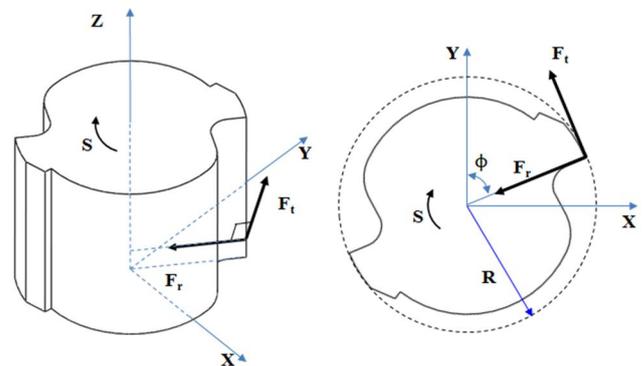
Fig. 7. Flat-end milling process with zero helix angle
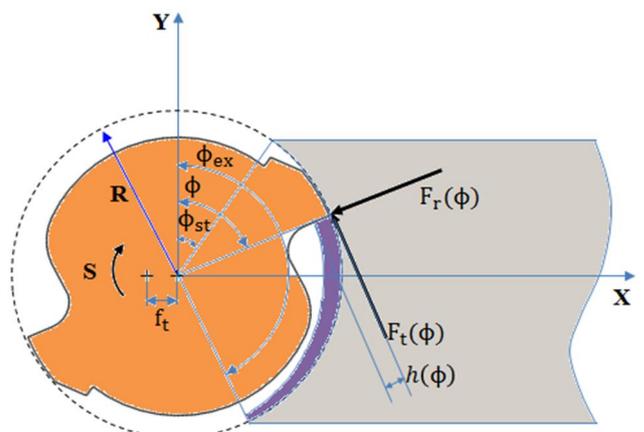
Fig. 8. Rotation angle in flat-end milling process with zero helix angle

In flat-end milling process with zero helix angle, the instantaneous chip thickness (h) varies periodically as a function of time-varying immersion (angle-varying

immersion); so, the instantaneous chip thickness can be calculated by Eq. (22) as shown in Fig. 7.

$$h(\phi) = f_t \sin \phi \qquad (22)$$

where f_t is the feed per tooth (the feed per flute) and ϕ is the instantaneous immersion angle.

In general, there are three components of cutting forces (tangential cutting force $F_t(\phi)$, radial cutting force $F_r(\phi)$, and axial cutting force $F_a(\phi)$) that can be expressed as a function of the varying uncut chip area and the contact length by Eq. (23) [2, 6].

$$\begin{cases} F_t(\phi) = K_{tc}ah(\phi) + K_{te}a \\ F_r(\phi) = K_{rc}ah(\phi) + K_{re}a \\ F_a(\phi) = K_{ac}ah(\phi) + K_{ae}a \end{cases} \qquad (23)$$

where a is the contact length (axial depth of cut) as shown in Fig. 9, $ah(\phi)$ is the uncut chip area, K_{tc} is the tangential shear force coefficient, K_{rc} is the radial shear force coefficient, K_{ac} is the radial shear force coefficient, and $K_{te}, K_{re},$ and K_{ae} are the tangential, radial, and axial edge force coefficients.
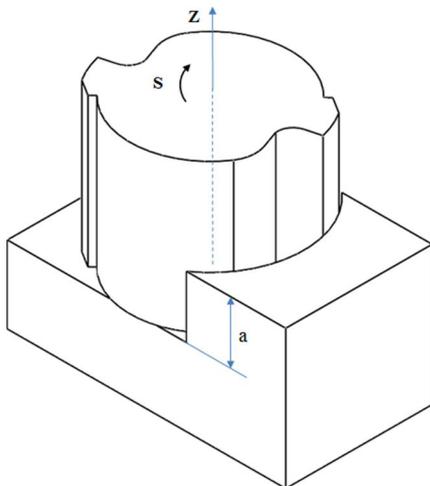
Fig. 9. The axial depth of cut in flat-end milling process with zero helix angle

It is assumed that nose radius and the approach angle on the inserts are zero and the helix angle is also zero, the axial components of cutting forces will become zero $(F_a(\phi) = 0)$. So, the feed, normal and axial cutting forces were described in Fig. 7 and can be calculated by Eq. (24).

$$\begin{cases} F_f(\phi) = -F_t \cos(\phi) - F_r \sin(\phi) \\ F_n(\phi) = +F_t \sin(\phi) - F_r \cos(\phi) \\ F_a(\phi) = 0 \end{cases} \qquad (24)$$

The cutting forces are produced only when the cutting tool is in the cutting zone as expressed by Eq. (25).

$$F_f(\phi), F_n(\phi) \neq 0 \text{ when } \phi_{st} \le \phi \le \phi_{ex} \qquad (25)$$

Considering the case more than one tooth cut simultaneously. The total feed and normal forces can be calculated by Eq. (26).

$$F_f(\phi) = \sum_{j=1}^{N_f} F_{f,j}(\phi_j), \quad F_n(\phi) = \sum_{j=1}^{N_f} F_{n,j}(\phi_j) \qquad (26)$$

where N_f is the number of flutes.

1.2.2. Cutting Force Modelling with Non-Zero Cutter Helix Angle

To dampen the sharp variations in the oscillatory components of the milling forces, the helical end-mills are used. They are often used when cutting with large depth of cut, but small width of cut. The geometry of a cutter with the helical flutes is described in Fig. 10.
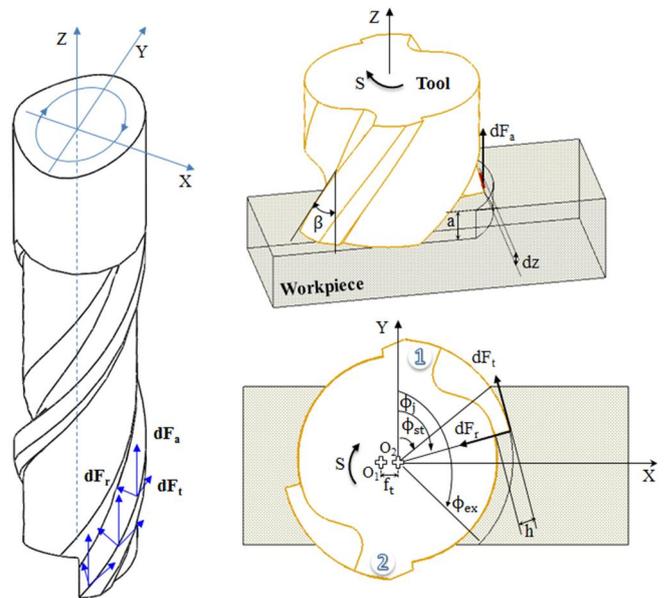
Fig. 10. Helical end-mill process

The helix angle of the helical cutter is β. On the effect of cutter's helix angle, a point (P) on the axis of cutting edge will be lagging behind the end point of the tool as shown in Fig. 11.
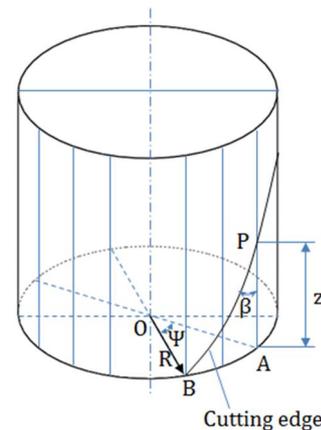
Fig. 11. The lag angle in helical end-mill

The lag angle (Ψ) at the axial depth of cut (z) can be calculated by Eq. (27).

$$AB = z * \tan \beta = R * \Psi = \frac{D}{2} * \Psi \qquad (27)$$

so

$$\Psi = \frac{2 \tan \beta}{D} z = k_b z \qquad (28)$$

where $k_b = \frac{2 \tan \beta}{D}$

The immersion is measured clockwise from the normal (y) axis. Assuming that the bottom end of one flute is designated as the reference immersion angle ϕ, the bottom endpoints of the remaining flutes are at angles $\phi_j(0)$ that can be calculated by Eq. (29).

$$\phi_j(0) = \phi + j\phi_p, j = 0,1, \dots (N-1) \qquad (29)$$

By the effect of cutter's helix angle, the immersion angle for flute j at axial depth of cut (z) is calculated by Eq. (30)

$$\phi_j(z) = \phi + j\phi_p - k_b z \qquad (30)$$

Tangential ($dF_{t,j}$), radial ($dF_{r,j}$), and axial ($dF_{a,j}$) forces acting on a differential flute element with height (dz) are expressed as Eq. (31), [12, 13, 14, 15].

$$\begin{cases} dF_{t,j}(\phi,z) = [K_{tc}h_j(\phi_j(z)) + K_{te}] * dz \\ dF_{r,j}(\phi,z) = [K_{rc}h_j(\phi_j(z)) + K_{re}] * dz \\ dF_{a,j}(\phi,z) = [K_{ac}h_j(\phi_j(z)) + K_{ae}] * dz \end{cases} \qquad (31)$$

where the chip thickness is calculated by Eq. (32).

$$h_j\left(\phi_j(z)\right) = f_t \sin\phi_j(z) \qquad (32)$$

By accepting the helix angle as the oblique angle of the mill (i = β), the elemental forces are resolved in the feed (x), normal (y), and axial (z) directions using the transformation as in Eq. (33).

$$\begin{cases} dF_{x,j}(\phi,z) = -dF_{t,j}(\phi,z)\cos\phi_j(z) \\ \qquad\qquad - dF_{r,j}(\phi,z)\sin\phi_j(z) \\ dF_{y,j}(\phi,z) = +dF_{t,j}(\phi,z)\sin\phi_j(z) \\ \qquad\qquad - dF_{r,j}(\phi,z)\cos\phi_j(z) \\ dF_{z,j}(\phi,z) = +dF_{a,j}(\phi,z) \end{cases} \qquad (33)$$

So,

$$\begin{cases} dF_{x,j}(\phi,z) = \left\{ \dfrac{f_t}{2}\begin{bmatrix} -K_{tc}\sin 2\phi_j(z) \\ -K_{rc}(1-\cos 2\phi_j(z)) \end{bmatrix} \\ \quad + [-K_{te}\cos\phi_j(z) - K_{re}\sin\phi_j(z)] \end{matrix}\right\} dz \\[4mm] dF_{y,j}(\phi,z) = \left\{ \dfrac{f_t}{2}\begin{bmatrix} K_{tc}\begin{matrix}(1-\cos 2\phi_j(z)) \\ -K_{rc}\sin 2\phi_j(z)\end{matrix} \end{bmatrix} \\ \quad + [K_{te}\sin\phi_j(z) - K_{re}\cos\phi_j(z)] \end{matrix}\right\} dz \\[4mm] dF_{z,j}(\phi,z) = \{K_{ac}f_t\sin\phi_j(z) + K_{ae}\}dz \end{cases} \qquad (34)$$

The differential cutting forces are integrated analytically along the in-cut portion of the flute j in obtaining the total cutting force produced by the flute as in Eq. (35).

$$\begin{aligned} F_q\left(\phi_j(z)\right) &= F_q(\phi,z) \\ &= \int_{z_{j,1}}^{z_{j,2}} dF_q(\phi,z), \quad q = x,y,z \end{aligned} \qquad (35)$$

where $z_{j,1}(\phi_j(z))$ and $z_{j,2}(\phi_j(z))$ are the lower and upper axial engagement limits of the in-cut portion of the flute j.

2. MODELLING OF VIBRATIONS IN MACHINING PROCESSES

2.1. Modelling of Vibrations in Turning Process

In the turning dynamic cutting process, at the time (t) the tool is removing the chip from an undulated surface that was generated during the previous pass when the tool vibrated with the amplitude in y direction ($y_{(t-\tau)}$) (outer modulation or wave removing). Besides, at the time (t), the tool is also vibrating with the amplitude ($y_{(t)}$) (inner modulation or wave generation). So, the orthogonal dynamic cutting process can be described as a superposition of these two distinct mechanisms as described in Fig. 12 [7].
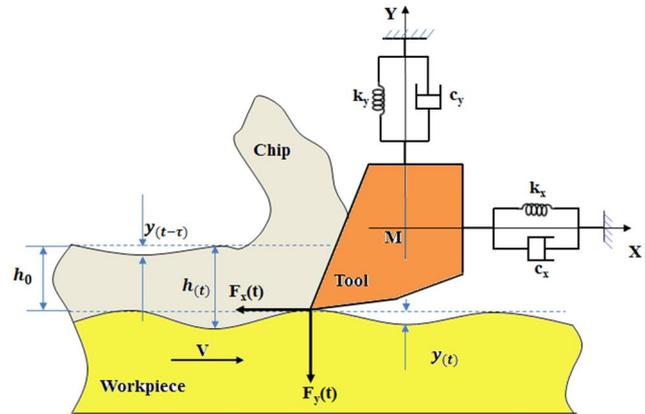
Fig. 12. Orthogonal dynamic cutting process

The traditional regenerative cutting force $F_y(t)$ at time t is expressed with velocity effect by Das and Tobias [8], Nguyen [9], and Altintas [10], and this model was expressed by Eq. (36) and Eq. (37).

$$\begin{cases} m_x\ddot{x}(t) + c_x\dot{x}(t) + k_x x = F_x(t) \\ m_y\ddot{y}(t) + c_y\dot{y}(t) + k_y y = F_y(t) \end{cases} \qquad (36)$$

$$\begin{cases} F_x(t) = K_f a[h_0 + x(t-\tau) - x(t)] - K_t a h_0 \dfrac{x}{v_y} \\ F_y(t) = K_f a[h_0 + y(t-\tau) - y(t)] - K_t a h_0 \dfrac{y}{v_x} \end{cases} \qquad (37)$$

where K_f and K_t are the static cutting force coefficients in feed and cutting speed directions, respectively. a is the width of cut, h_0 is the uncut chip thickness, V is the cutting velocity, and τ is the time delay between the inner and outer vibration waves.

Many studies were performed to investigate the dynamic cutting processes and analyze the stability lobes in orthogonal cutting and turning processes such as Altintas et al [10], Budak and Ozlu [11], Ahmadi and Ismail [12], Otto et al [13].

2.2. Modelling of Vibrations in Milling Process

In the static models of cutting force, the structural vibrations during cutting process are ignored. In fact, the milling process is the dynamic milling process that includes the effect of structural vibrations during cutting process. In dynamic milling, the periodic cutting forces can cause forced vibrations in milling system. Under some conditions, force induced vibrations may be inherent in the cutting process at the tooth passing frequency. For other conditions, the vibration may cause the cutting process to vary as shown in Fig. 13 [7].

In the dynamic milling processes, the dynamic chip thickness and cutting forces were analyzed to predict the

vibrations and the chatter frequency. Many studies were performed to analyze the stability lobes in milling processes such as Altintas [2], Altintas and Lee [14], Budak [15, 16], Moradi et al [17], Govekar et al [18].

Milling process is a dynamic process; so, by the effect of machine tool dynamic structure, the machine tool vibrations in x and y directions were calculated by Eq. (38), [7, 9, 13, 19].
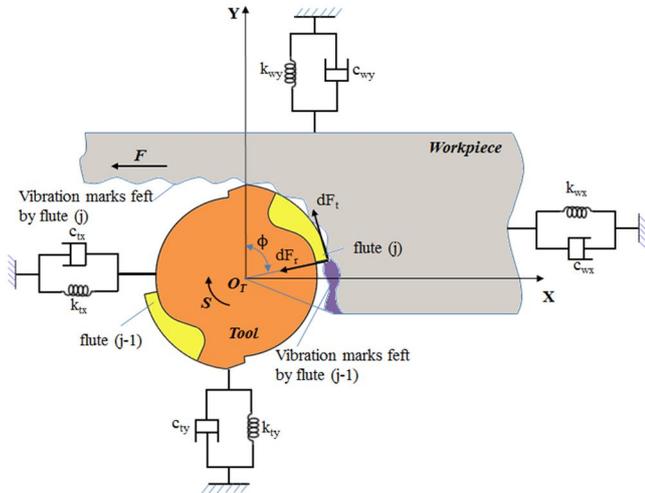
Fig. 13. Dynamic milling process

$$\begin{cases} m_x\ddot{x}(t) + c_x\dot{x}(t) + k_x x = F_x(t) \\ m_y\ddot{y}(t) + c_y\dot{y}(t) + k_y y = F_y(t) \\ m_z\ddot{z}(t) + c_z\dot{z}(t) + k_z z = F_z(t) \end{cases} \qquad (38)$$

Finally, the dynamic cutting forces were simulated following the block diagram in Fig. 14 [7]. The simulation procedure starts from static chip thickness and cutter run-out model. The cutting forces are calculated for the cutting processes based on the cutting force coefficients, the cutting conditions, and cutting force models. That process is called the cutting process.
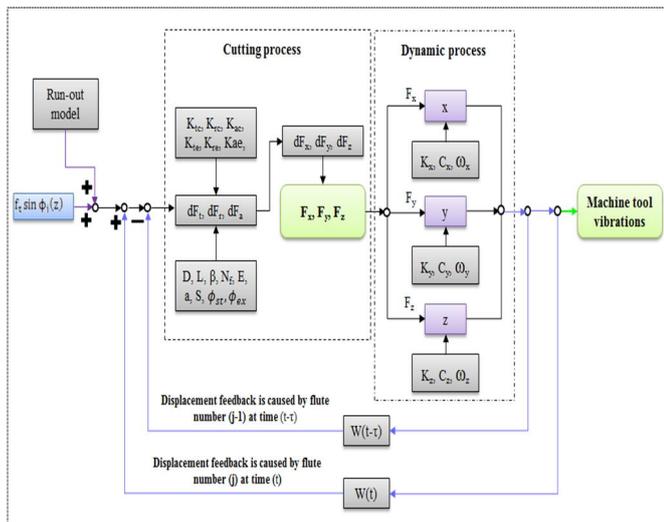
Fig. 14. Block diagram of the integrated prediction procedures of dynamic cutting forces

In the dynamic process, the machine tool vibrations are generated by the effect of cutting forces and the machine tool dynamic structure. By the effect of machine tool vibrations in x and y directions, the chip thickness changes as the dynamic chip thickness, and the calculation process of cutting force is repeated as a new loop. This calculation process is a closed loop. By using this process, the cutting force in tangential, radial, and axial directions could be determined.

3. REVIEW OF EXPERIMENTAL METHODS IN INVESTIGATION OF CUTTING FORCES AND MACHINING VIBRATIONS

Using the keyword "Cutting force" to search in google scholar, about 3,540,000 results were found in 0.06 seconds. Similarly, using the keyword "Vibrations", there are about 3,560,000 results that were found in 0.03 seconds of searching time. There are a lot of studies about cutting forces and vibrations. Al most of these studies were conducted by using force and vibration measurement systems. The cutting force measurement system can be used to measure the cutting force in machining processes such as milling, turning, etc. as shown in Fig. 15 [6].

a. CNC machine
b. Dynamometer
d. Signal Filter and Processing System
d. PC and Display System

Fig. 15. Setup measurement of cutting force setting

The vibration measurement system can be applied to measure the machine-tool vibrations, workpiece vibrations, the parameters of machine-tool dynamic structure and workpiece dynamic structure, and so. on as shown in Fig. 16 [20].

a. Tool   b. Acceleration sensor   c. Force sensor
d. Signal processing box   e. PC and CUTPROTM software
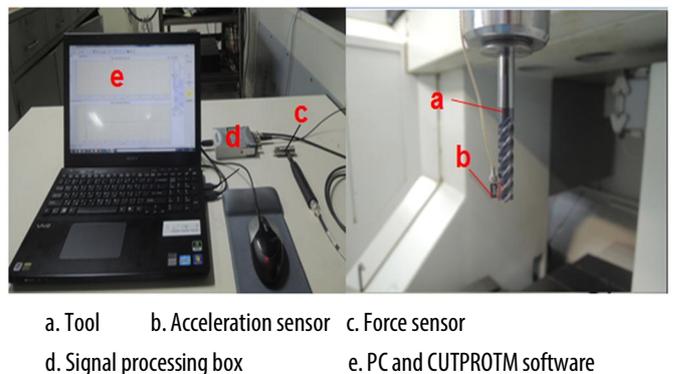
Fig. 16. Setup of FRF measurement

The above measurement systems can be applied to measure the cutting forces, vibrations, machine-tool dynamic structure for different pairs of tool and workpiece.

4. REVIEW OF THE INVESTIGATED RESULTS

4.1. Verification of Cutting Force Models in Machining Processes

The dynamometer and measurement system were often used to measure the cutting forces in machining processes. In the Fig. 17 [6], the investigated results that showed the comparison of measured and predicted cutting forces in a flat end mill process. The compared results that were the basic to withdraw the conclusions of each study. So, the cutting force measurement system is an important system that was used to verify the proposed models of cutting force and to evaluate the accuracy of each prediction model.
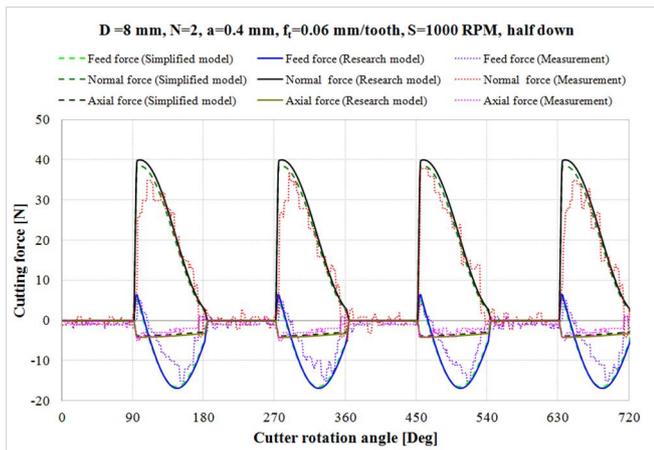
Fig. 17. Verification of simulation results

4.2. Investigation of Machine-Tool Dynamic Structure

By using the measured results of forces and vibrations, the signal of hammer force and the acceleration values obtained from the force and acceleration sensors are shown in the time domain of a machine-tool system. And then, the machine tool dynamic structure was analysed by the modals in x and y directions. Finally, the parameters of the machine tool dynamic structure were determined for a machine tool system and listed in Table 1 [9].

Table 1. Machine tool dynamic structure parameters

Direction	Mode No	Natural Frequency [Hz]	Damping Ratio [%]	Modal Stiffness [N/m]	Mass [kg]
X	1	842.9752	0.898	7.8919E+08	28.1316
	2	1591.7397	5.067	4.8211E+07	0.4820
	3	2790.6410	3.940	1.2730E+07	0.0414
Y	1	991.8001	2.641	1.8614E+08	4.7933
	2	1514.4826	6.180	4.0318E+07	0.4453
	3	2785.8612	6.635	1.3818E+07	0.0451

4.3. Prediction of Machine-Tool Vibrations

Using the measured results of forces and vibrations, the parameters of machine-tool dynamic structure were determined. And then, the cutting force models can be extended to predict the models of other machining characteristics such as machine-tool vibrations as shown in

Fig. 18 [9]. However, it seems that the vibration models have not been verified in previous studies, so, it is necessary to perform the next studies to verify the machine-tool vibration models and to evaluate the accuracy of a proposed vibration models.
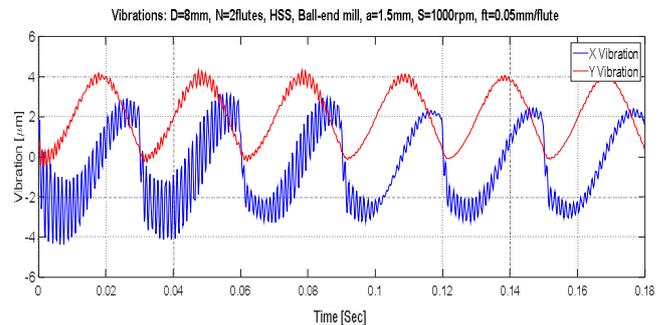
Fig. 18. The predicted result of machine tool vibrations

5. CONCLUSION

In this study, the review of cutting force and vibration modelling was presented. By analysis of results from previous studies, the conclusions of this study can be listed as following.

- Cutting force and vibration modelling were significant works that were performed by many researchers to predict the cutting forces and machine - tool vibrations, and to improve the quality of machining processes.

- In machining processes, cutting forces can be modelled by orthogonal and oblique cutting processes that include turning, milling and other machining processes.

- Cutting force and vibration measurement systems can be used to measure the cutting forces, machine-tool vibrations, to verify and evaluate the accuracy of the proposed cutting force and vibration models.

- Development and verification of cutting force models, vibration models, surface error models, etc. prediction and optimization of machining processes are the proposed research directions of this study.

REFERENCES

[1]. Merchant M. E., 1945. *Mechanics of the metal cutting process. I. Orthogonal cutting and a type 2 chip.* Journal of applied physics, 16(5), 267-275.

[2]. Altintas Y., 2012. *Manufacturing automation: metal cutting mechanics, machine tool vibrations, and CNC design.* Cambridge university press.

[3]. Budak E., Altintas Y., Armarego E. J. A., 1996. *Prediction of milling force coefficients from orthogonal cutting data.* Journal of Manufacturing Science and Engineering, 118(2), 216-224.

[4]. Altintas Y., 2000. *Modeling approaches and software for predicting the performance of milling operations at MAL-UBC.* Machining science and technology, 4(3), 445-478.

[5]. Zorev N. N., 1963. *Inter-relationship between shear processes occurring along tool face and shear plane in metal cutting.* International Research in Production Engineering, Vol. 49.

SCIENCE - TECHNOLOGY

[6]. Kao Y. C., Nguyen N. T., Chen M. S., Su S. T., 2015. *A prediction method of cutting force coefficients with helix angle of flat-end cutter and its application in a virtual three-axis milling simulation system.* The International Journal of Advanced Manufacturing Technology, 77(9-12), 1793-1809.

[7]. Nguyen Nhu Tung, 2020. *Modeling of the Machining Dynamics: Cutting forces and Machining Characteristics in Three-Axis Milling Processes.* Science and Technics Publishing House, ISBN: 978-604-67-17584-4.

[8]. Das M. K., Tobias S. A., 1967. *The relation between the static and the dynamic cutting of metals.* International Journal of Machine Tool Design and Research, 7(2), 63-89.

[9]. Nguyen Nhu-Tung, Yung-Chou Kao, Hoang Tien Dung, 2019. *A Prediction Method of Dynamic Cutting Forces and Machine-Tool Vibrations When Milling by Using Ball-End Mill Cutter.* In International Conference on Engineering Research and Applications, pp. 47-54. Springer, Cham.

[10]. Altintas Y., Eynian M., Onozuka H., 2008. *Identification of dynamic cutting force coefficients and chatter stability with process damping.* CIRP Annals-Manufacturing Technology, 57(1), 371-374.

[11]. Budak E., Ozlu E., 2007. *Analytical modeling of chatter stability in turning and boring operations: a multi-dimensional approach.* CIRP Annals-Manufacturing Technology, 56(1), 401-404.

[12]. Ahmadi K., Ismail F., 2011. *Analytical stability lobes including nonlinear process damping effect on machining chatter.* International Journal of Machine Tools and Manufacture, 51(4), 296-308.

[13]. Otto A., Rauh S., Kolouch M., Radons G., 2014. *Extension of Tlusty′s law for the identification of chatter stability lobes in multi-dimensional cutting processes.* International Journal of Machine Tools and Manufacture, 82, 50-58.

[14]. Altintaş Y., Lee P., 1996. *A general mechanics and dynamics model for helical end mills.* CIRP Annals-Manufacturing Technology, 45(1), 59-64.

[15]. Budak E., 2006. *Analytical models for high performance milling. Part II: Process dynamics and stability.* International Journal of Machine Tools and Manufacture, 46(12), 1489-1499.

[16]. Budak E., 2003. *An analytical design method for milling cutters with nonconstant pitch to increase stability, part I: theory.* Transactions American society of mechanical engineer journal of manufacturing science and engineering, Vol. 125(1), 29-34.

[17]. Moradi H., Vossoughi G., Movahhedy M. R., 2013. *Experimental dynamic modelling of peripheral milling with process damping, structural and cutting force nonlinearities.* Journal of Sound and Vibration, 332(19), 4709-4731.

[18]. Govekar E., Gradišek J., Kalveram M., Insperger T., Weinert K., Stépàn G., Grabec I. (2005). *On stability and dynamics of milling at small radial immersion.* CIRP Annals-Manufacturing Technology, 54(1), 357-362.

[19]. Balachandran B., Gilsinn D., 2005. *Non-linear oscillations of milling.* Mathematical and Computer Modelling of Dynamical Systems, 11(3), 273-290.

[20]. Nhu-Tung Nguyen, Van-Nam Hoang, Anh-Tuan Do, Huu-Hung Nguyen, 2019. *A combination method of theory and experimental in determination of machine-tool dynamic structure parameters.* Journal of Science and Technology - Hanoi University of Industry, 52(6), ISSN: 1859-3585.

THÔNG TIN TÁC GIẢ

Nguyễn Như Tùng, Hoàng Tiến Dũng, Phạm Văn Đông, Đỗ Đức Trung, Bùi Văn Bảo

Trường Đại học Công nghiệp Hà Nội